Data Analysis

Parametric data such as body weight, food consumption, urinalysis findings (urine volume and osmotic pressure), hematologic and biochemical findings, and organ weights were analyzed by Bartlett's test (Bartlett, 1937) for homogeneity of distribution. When homogeneity was recognized, Dunnett's test (Dunnett, 1964) was conducted for comparison between control and individual treatment groups. If not homogenous, the data were analyzed using Steel's multiple comparison test (Steel, 1959). For histopathologic findings, Fisher's exact test (Fisher, 1973) was performed. The 5% level of probability was used as the criterion for significance.

RESULTS

No death or clinical sings of toxicity were found in any groups. There were also no significant changes in body weight, but a significant increase in food consumption was noted on dosing days 14 and 21 in males and on dosing days 21 and 27 in females at 62.5 mg/kg. No dose-related changes were found in the findings of urinalysis.

At the end of the 28-day administration period, a significant decrease in red blood cell count, hematocrit and hemoglobin at 2.5 mg/kg and more, decrease in MCHC at 12.5 mg/kg and more, and increase in platelet count at 62.5 mg/kg were noted in males, but these changes were not found in females (Table 1). For clotting factors, a significant decrease in fibrinogen was noted at 2.5 mg/kg and more in males and at 62.5 mg/kg in females (Table 1) but no significant prolongation of PT or APTT.

Blood biochemical examination revealed significant increases in the A/G ratio at 0.5 mg/kg and more, and levels of glucose at 2.5 mg/kg and more, albumin, ALT, and ALP at 12.5 mg/kg and more, and BUN and AST at 62.5 mg/kg in males (Table 2). On the other hand, for females, a significant increase in the levels of glucose, A/G ratio, total cholesterol, triglyceride, and ALT was noted only at 62.5 mg/kg.

At necropsy, absolute liver weight was significantly increased at 2.5 mg/kg and more in males and at 12.5 mg/kg and more in females with a significant increase in the relative weight at all doses in males and at 12.5 mg/kg and more in females (Table 3). In the highest dose group, there was also a significant increase in absolute and relative kidney weight in males and in absolute heart weight in females. No test-substance-related significant change was detected in other organs. Macroscopically, enlargement of the liver was observed at all doses in males and at 12.5 mg/kg and more in females. In the liver, a white patch/zone was found at 2.5 mg/kg and more in males and at 62.5 mg/kg in females.

Table 1: Principal hematologic values in male and female rats given HDBB by gavage for 28 days.

	At the completion of the administration period					At the completion of the recovery period	
	0 mg kg^{-1} day^{-1}	0.5 mg kg^{-1} day^{-1}	2.5 mg kg^{-1} day^{-1}	12.5 mg kg^{-1} day^{-1}	62.5 mg kg^{-1} day^{-1}	0 mg kg^{-1} day^{-1}	62.5 mg kg^{-1} day^{-1}
Male							
No. of animals	5	5	5	5	5	5	5
Red blood cells (10^6/mm^3)	7.89 ± 0.18	7.65 ± 0.32	7.23 ± 0.33*	7.18 ± 0.27**	7.16 ± 0.46**	8.26 ± 0.16	7.65 ± 0.38*
Hemoglobin (g/dL)	15.2 ± 0.4	14.8 ± 0.5	13.9 ± 0.8**	13.6 ± 0.3**	13.2 ± 0.3**	15.3 ± 0.3	13.2 ± 0.9**
Hematocrit (%)	45.6 ± 1.8	44.6 ± 1.5	42.5 ± 2.4*	41.9 ± 1.2**	40.7 ± 0.9**	44.6 ± 1.0	40.1 ± 2.7**
MCV (μm^3)	57.8 ± 1.9	58.3 ± 1.5	58.7 ± 1.2	58.3 ± 1.7	57.0 ± 2.7	54.0 ± 1.6	52.5 ± 2.6
MCH (pg)	19.3 ± 0.7	19.4 ± 0.6	19.3 ± 0.4	19.0 ± 0.9	18.4 ± 0.9	18.5 ± 0.5	17.3 ± 0.9*
MCHC (%)	33.4 ± 0.7	33.2 ± 0.5	32.8 ± 0.2	32.5 ± 0.7*	32.3 ± 0.3*	34.2 ± 0.3	32.9 ± 0.6**
Reticulocyte (%)	2.8 ± 0.3	3.3 ± 0.4	3.2 ± 0.3	3.9 ± 0.5*	3.2 ± 1.0	2.5 ± 0.4	4.4 ± 0.2**
Platelet count (10^3/mm^3)	1202 ± 75	1265 ± 107	1280 ± 116	1572 ± 430	1639 ± 227*	1196 ± 145	1502 ± 134**
Fibrinogen (mg/dL)	249 ± 13	224 ± 8	189 ± 15**	198 ± 21**	193 ± 20**	240 ± 24	214 ± 13
Female							
No. of animals	5	5	5	5	5	5	5
Red blood cells (10^6/mm^3)	7.81 ± 0.38	7.62 ± 0.61	7.79 ± 0.22	7.46 ± 0.30	7.49 ± 0.30	7.80 ± 0.27	7.64 ± 0.38
Hemoglobin (g/dL)	15.1 ± 0.9	14.9 ± 1.3	15.2 ± 0.4	14.8 ± 0.7	14.1 ± 0.6	14.9 ± 0.5	14.2 ± 0.6
Hematocrit (%)	43.7 ± 1.7	43.5 ± 3.1	44.0 ± 1.3	43.1 ± 1.8	41.6 ± 1.6	42.2 ± 1.0	40.6 ± 1.6
MCV (μm^3)	56.0 ± 1.1	57.1 ± 1.6	56.4 ± 0.8	57.7 ± 1.4	55.6 ± 1.0	54.2 ± 0.8	53.2 ± 1.8
MCH (pg)	19.3 ± 0.4	19.6 ± 0.6	19.5 ± 0.4	19.8 ± 0.5	18.9 ± 0.4	19.1 ± 0.3	18.6 ± 0.6
MCHC (%)	34.5 ± 0.8	34.3 ± 0.8	34.5 ± 0.4	34.4 ± 0.3	34.0 ± 0.4	35.2 ± 0.3	35.1 ± 0.4
Reticulocyte (%)	2.1 ± 0.4	3.5 ± 1.7	2.6 ± 0.4	2.5 ± 0.2	2.4 ± 0.3	2.7 ± 0.4	2.6 ± 0.3
Platelet count (10^3/mm^3)	1295 ± 118	1360 ± 155	1367 ± 79	1368 ± 138	1350 ± 194	1166 ± 64	1410 ± 95**
Fibrinogen (mg/dL)	193 ± 11	222 ± 46	186 ± 9	184 ± 29	155 ± 10*	210 ± 7	241 ± 7**

Values are expressed as the mean ± SD.
*Significantly different from the control, $p \leq 0.05$.
**Significantly different from the control, $p \leq 0.01$.

Table 2: Principal blood biochemical values in male and female rats given HDBB by gavage for 28 days.

	At the completion of the administration period					At the completion of the recovery period	
	0 mg kg^{-1} day^{-1}	0.5 mg kg^{-1} day^{-1}	2.5 mg kg^{-1} day^{-1}	12.5 mg kg^{-1} day^{-1}	62.5 mg kg^{-1} day^{-1}	0 mg kg^{-1} day^{-1}	62.5 mg kg^{-1} day^{-1}
Male							
No. of animals	5	5	5	5	5	5	5
Total protein (g/dL)	5.84 ± 0.34	5.52 ± 0.10	5.55 ± 0.24	5.72 ± 0.22	5.86 ± 0.40	6.02 ± 0.19	5.95 ± 0.49
Albumin (g/dL)	3.78 ± 0.22	3.90 ± 0.17	4.06 ± 0.20	4.43 ± 0.18**	4.40 ± 0.41**	3.75 ± 0.1	4.22 ± 0.45*
A/G ratio	1.85 ± 0.18	2.43 ± 0.23*	2.75 ± 0.29**	3.47 ± 0.25**	3.05 ± 0.55**	1.66 ± 0.11	2.46 ± 0.34*
Glucose (mg/dL)	122 ± 13	132 ± 15	170 ± 18**	170 ± 10**	156 ± 16**	166 ± 13	182 ± 22
Total cholesterol (mg/dL)	59 ± 11	46 ± 9	45 ± 4	49 ± 13	52 ± 20	62 ± 13	55 ± 19
Triglyceride (mg/dL)	25.5 ± 8.4	24.3 ± 4.5	34.5 ± 7.1	44.8 ± 20.9	45.8 ± 12.5	68.0 ± 52.0	47.5 ± 26.6
BUN (mg/dL)	13.0 ± 2.5	12.9 ± 0.5	15.5 ± 1.7	15.8 ± 1.3	17.2 ± 2.4**	14.5 ± 2.4	19.0 ± 1.9*
AST (U/L)	72 ± 7	71 ± 11	65 ± 5	83 ± 22	115 ± 16*	61 ± 7	68 ± 22
ALT (U/L)	30 ± 5	28 ± 4	32 ± 3	42 ± 5*	48 ± 10**	25 ± 5	49 ± 29**
ALP (U/L)	757 ± 175	992 ± 220	1089 ± 168	1569 ± 427**	1462 ± 250**	622 ± 123	906 ± 169*
Female							
No. of animals	5	5	5	5	5	5	5
Total protein (g/dL)	5.68 ± 0.14	5.61 ± 0.18	5.53 ± 0.19	5.93 ± 0.33	5.85 ± 0.19	5.91 ± 0.29	6.50 ± 0.30*
Albumin (g/dL)	3. 81 ± 0.23	3.67 ± 0.43	3.72 ± 0.12	4.12 ± 0.14	4.21 ± 0.18	3.85 ± 0.32	4.27 ± 0.10*
A/G ratio	2.04 ± 0.26	1.95 ± 0.44	2.09 ± 0.27	2.30 ± 0.25	2.59 ± 0.29*	1.89 ± 0.25	1.93 ± 0.18
Glucose (mg/dL)	110 ± 15	120 ± 20	114 ± 16	127 ± 22	151 ± 8**	117 ± 8	149 ± 16**
Total cholesterol (mg/dL)	49 ± 10	59 ± 5	50 ± 7	54 ± 6	84 ± 16**	63 ± 6	91 ± 14**
Triglyceride (mg/dL)	12.3 ± 5.6	12.1 ± 2.6	8.8 ± 3.7	12.2 ± 1.1	31.9 ± 4.8**	18.8 ± 7.6	37.7 ± 18.8
BUN (mg/dL)	16.1 ± 4.3	15.5 ± 1.5	16.6 ± 3.8	15.8 ± 2.4	16.9 ± 1.3	16.6 ± 1.2	16.8 ± 0.8
AST (U/L)	68 ± 5	69 ± 11	66 ± 7	68 ± 9	76 ± 12	66 ± 13	65 ± 19
ALT (U/L)	21 ± 2	22 ± 4	23 ± 3	27 ± 4	33 ± 6**	25 ± 4	36 ± 21
ALP (U/L)	490 ± 110	409 ± 86	414 ± 85	433 ± 83	633 ± 199	381 ± 138	247 ± 63

Values are expressed as the mean ± SD.
*Significantly different from the control, $p \leq 0.05$.
**Significantly different from the control, $p \leq 0.01$.

Table 3: Principal organ weights of male and female rats given HDBB by gavage for 28 days.

	At the completion of the administration period					At the completion of the recovery period	
	0 mg kg^{-1} day^{-1}	0.5 mg kg^{-1} day^{-1}	2.5 mg kg^{-1} day^{-1}	12.5 mg kg^{-1} day^{-1}	62.5 mg kg^{-1} day^{-1}	0 mg kg^{-1} day^{-1}	62.5 mg kg^{-1} day^{-1}
Male							
No. of animals	5	5	5	5	5	5	5
Brain (g)	2.02 ± 0.08	2.03 ± 0.07	2.12 ± 0.06	2.08 ± 0.05	2.06 ± 0.09	2.10 ± 0.10	2.07 ± 0.10
	(0.624 ± 0.009)[a]	(0.622 ± 0.038)	(0.633 ± 0.062)	(0.628 ± 0.044)	(0.630 ± 0.046)	(0.527 ± 0.046)	(0.580 ± 0.034)
Heart (g)	1.09 ± 0.09	1.10 ± 0.11	1.17 ± 0.14	1.18 ± 0.07	1.23 ± 0.19	1.20 ± 0.10	1.28 ± 0.16
	(0.337 ± 0.026)	(0.336 ± 0.028)	(0.346 ± 0.011)	(0.355 ± 0.017)	(0.374 ± 0.028)	(0.298 ± 0.008)	(0.356 ± 0.016**)
Liver (g)	9.40 ± 0.58	11.65 ± 1.90	17.11 ± 3.46*	21.64 ± 2.73*	24.47 ± 5.06*	11.8 ± 1.64	20.61 ± 3.36**
	(2.908 ± 0.139)	(3.533 ± 0.296*)	(5.045 ± 0.506*)	(6.507 ± 0.536*)	(7.413 ± 1.283*)	(2.930 ± 0.133)	(5.746 ± 0.527**)
Kidneys (g)	2.43 ± 0.22	2.54 ± 0.17	2.74 ± 0.29	2.88 ± 0.40	3.04 ± 0.45*	2.83 ± 0.23	2.91 ± 0.40
	(0.753 ± 0.075)	(0.775 ± 0.046)	(0.814 ± 0.053)	(0.865 ± 0.080)	(0.927 ± 0.119**)	(0.706 ± 0.046)	(0.814 ± 0.066*)
Testes (g)	2.90 ± 0.16	2.84 ± 0.12	2.88 ± 0.15	2.91 ± 0.15	2.92 ± 0.14	3.13 ± 0.11	3.07 ± 0.18
	(0.901 ± 0.080)	(0.871 ± 0.084)	(0.865 ± 0.121)	(0.879 ± 0.046)	(0.891 ± 0.068)	(0.787 ± 0.099)	(0.861 ± 0.043)
Female							
No. of animals	5	5	5	5	5	5	5
Brain (g)	1.94 ± 0.10	1.92 ± 0.08	1.95 ± 0.07	1.90 ± 0.12	1.90 ± 0.03	1.99 ± 0.02	1.94 ± 0.05
	(0.931 ± 0.053)	(0.884 ± 0.012)	(0.901 ± 0.052)	(0.857 ± 0.046)	(0.841 ± 0.058*)	(0.838 ± 0.086)	(0.802 ± 0.084)
Heart (g)	0.75 ± 0.07	0.77 ± 0.03	0.75 ± 0.02	0.78 ± 0.05	0.84 ± 0.06*	0.79 ± 0.04	0.87 ± 0.06
	(0.357 ± 0.019)	(0.356 ± 0.008)	(0.348 ± 0.007)	(0.351 ± 0.009)	(0.371 ± 0.024)	(0.333 ± 0.022)	(0.357 ± 0.028)
Liver (g)	6.39 ± 0.87	6.84 ± 0.63	6.73 ± 0.26	8.67 ± 1.16**	12.43 ± 0.89**	6.80 ± 0.86	8.85 ± 0.99**
	(3.053 ± 0.178)	(3.146 ± 0.197)	(3.112 ± 0.107)	(3.885 ± 0.324**)	(5.497 ± 0.172**)	(2.836 ± 0.076)	(3.626 ± 0.117**)
Kidneys (g)	1.70 ± 0.14	1.61 ± 0.08	1.71 ± 0.09	1.72 ± 0.11	1.87 ± 0.19	1.77 ± 0.18	1.86 ± 0.13
	(0.816 ± 0.057)	(0.742 ± 0.033*)	(0.789 ± 0.029)	(0.776 ± 0.040)	(0.827 ± 0.042)	(0.744 ± 0.075)	(0.766 ± 0.070)
Ovaries (mg)	87 ± 22	96 ± 18	82 ± 11	97 ± 9	89 ± 18	88 ± 12	101 ± 11
	(0.041 ± 0.007)	(0.044 ± 0.008)	(0.038 ± 0.005)	(0.044 ± 0.005)	(0.039 ± 0.008)	(0.037 ± 0.004)	(0.041 ± 0.003)

Values are expressed as the mean ± SD.
[a] Relative organ weight (organ weight per body weight) (%).
*Significantly different from the control, $p \leq 0.05$.
**Significantly different from the control, $p \leq 0.01$.

On histopathology, test-substance-related changes were observed in the liver, heart, kidneys, thyroids, and spleen as shown in Table 4. In the liver, hypertrophy of hepatocytes in males at 0.5 mg/kg and more and in females at 12.5 and 62.5 mg/kg; bile duct proliferation and decreased incidence of hepatocellular fatty change in males at 0.5 mg/kg and more and in females at 62.5 mg/kg; vacuolar degeneration of hepatocytes in males at 2.5 mg/kg and more and in females at 62.5 mg/kg; focal necrosis in males at 2.5 mg/kg and more; increased mitosis of hepatocytes in males at 62.5 mg/kg and in females at 12.5 and 62.5 mg/kg; and hepatocellular pigmentation and/or cytoplasmic inclusion bodies in males at 62.5 mg/kg were observed. In the heart, cell infiltration at 2.5 mg/kg and more in males, and degeneration and/or hypertrophy of the myocardium at 12.5 and 62.5 mg/kg in both sexes were noted. Furthermore, hypertrophy of the tubular epithelium was observed in the kidneys of males at 12.5 and 62.5 mg/kg and of females at 62.5 mg/kg, and increased severity of basophilic tubules was found in males at 62.5 mg/kg. In the thyroids and spleen, diffuse follicular cell hyperplasia at 62.5 mg/kg in both sexes and extramedullary hematopoiesis at 2.5 mg/kg and more in males, respectively, were detected.

At the end of the recovery period, a significant decrease in red blood cell count, hematocrit, hemoglobin and MCHC, and increase in platelet count were still observed in males, and a significant decrease in MCH and increase in reticulocyte in males and increase in platelet count in females were additionally found (Table 1). A significant increase in serum levels of albumin, A/G ratio, BUN, ALT, and ALP in males, and in total protein, albumin, glucose and total cholesterol in females was also noted (Table 2). At necropsy, grossly enlarged liver was still observed, and the absolute and relative weight was significantly increased in both sexes (Table 3). In males, the liver was brown, and some were accompanied with a red or white patch/zone. A significant increase in the relative weight of the heart and kidneys was also noted in males (Table 3). Histopathologically, except for increased mitosis of hepatocytes, hepatic changes were observed with similar incidence as observed at the end of the administration period in males (Table 4). Degeneration of the myocardium and cell infiltration in the heart, diffuse follicular cell hyperplasia in the thyroid, and extramedullary hematopoiesis in the spleen were also detected in males. In females, hypertrophy of hepatocytes was found, but other histopathologic changes observed at the end of the administration period were not detected. In the liver, focal necrosis and hepatocellular pigmentation were also found in females.

DISCUSSION

The current study was conducted to obtain initial information on the possible repeated-dose toxicity of HDBB in rats. The dosage of HDBB used in this

Table 4: Histopathologic findings in the principal organs of male and female rats given HDBB by gavage for 28 days.

		At the completion of the administration period					At the completion of the recovery period	
	Grade	0 mg kg^{-1} day^{-1}	0.5 mg kg^{-1} day^{-1}	2.5 mg kg^{-1} day^{-1}	12.5 mg kg^{-1} day^{-1}	62.5 mg kg^{-1} day^{-1}	0 mg kg^{-1} day^{-1}	62.5 mg kg^{-1} day^{-1}
Male								
No. of animals		5	5	5	5	5	5	5
Liver								
Hypertrophy of hepatocytes	+	0	3	5**	5**	5**	0	5**
Fatty change of hepatocytes	+	5	0**	0**	0**	0**	5	0**
Bile duct proliferation	+	0	1	1	4*	4*	0	4*
Vacuolar degeneration of hepatocytes	+	0	0	5**	5**	5**	0	4*
Focal necrosis	+	0	0	1	2	4*	0	3
Increased mitosis of hepatocytes	+	0	0	0	0	4*	0	0
Pigment deposit of hepatocytes	+	0	0	0	0	1	0	2
Cytoplasmic inclusion bodies	+	0	0	0	0	1	0	1
Heart								
Cell infiltration	+	0	1	5**	4*	4*	1	3
Degeneration of myocardium	+	0	0	0	5**	5**	0	4*
Hypertrophy of myocardium	+	0	0	0	3	4*	0	0
Kidney								
Hypertrophy of tubular epithelium	+	0	0	0	2	5**	0	0
Basophilic tubules	+	2	3	4	3	3	4	4
	++	0	0	0	0	2	0	0
Thyroid								
Diffuse follicular cell hyperplasia	+	0	0	0	0	2	0	3

Spleen								
Extramedullary hematopoiesis	+	0	0	3	2	2	0	3
Female								
No. of animals		5	5	5	5	5	5	5
Liver								
Hypertrophy of hepatocytes	+	0	0	0	5**	5**	0	3
Fatty change of hepatocytes	+	5	5	5	3	0**	5	4
Bile duct proliferation	+	0	0	0	0	1	0	0
Vacuolar degeneration of hepatocytes	+	0	0	0	0	2	0	0
Focal necrosis	+	0	0	0	0	0	0	2
Increased mitosis of hepatocytes	+	0	0	0	1	2	0	0
Pigment deposit of hepatocytes	+	0	0	0	0	0	0	1
Heart								
Cell infiltration	+	0	1	0	0	1	0	0
Degeneration of myocardium	+	0	0	0	3	5**	0	0
Hypertrophy of myocardium	+	0	0	0	1	3	0	0
Kidney								
Hypertrophy of tubular epithelium	+	0	0	0	0	2	0	0
Basophilic tubules	+	1	2	2	0	3	4	4
Thyroid								
Diffuse follicular cell hyperplasia	+	0	0	0	0	2	0	0
Spleen								
Extramedullary hematopoiesis	+	0	1	0	0	0	0	0

Values represent the number of animals with findings.
+: slight; ++: moderate.
*Significantly different from the control, $p \leq 0.05$.
**Significantly different from the control, $p \leq 0.01$.

study was sufficiently high to be expected to induce toxicity in the liver. As expected, histopathologic changes including vacuolar degeneration and hypertrophy of hepatocytes were observed in the liver. These findings showed that one of the toxicologically main targets of HDBB was the liver. Increased food consumption without body weight changes, increased blood glucose, total cholesterol and triglyceride, and decreased incidence of fatty changes of hepatocytes were noted after HDBB administration for 28 days. These changes indicate metabolic derangement and suggest possible adverse effects of HDBB in metabolic homeostasis. The current study showed that the heart was another toxicologic target organ for HDBB. Although degeneration and hypertrophy of the myocardium and cell infiltration were observed after HDBB administration, cardiac function was not evaluated in the current study. Further studies are required to clarify the adverse effects of HDBB on cardiac function, because functional parameters are considered to be more susceptible than histopathologic changes in the heart (Glaister, 1992). In our study, HDBB also caused anemic changes (decreased red blood cell count, hematocrit, hemoglobin and MCHC, and extramedullary hematopoiesis), and adverse effects on the kidneys (hypertrophy of tubular epithelium and increased severity of basophilic tubules with increased BUN) and the thyroids (diffuse follicular cell hyperplasia) at higher doses. Adverse effects on the liver and kidneys, and anemia, but not adverse effects on the heart and thyroid, were reported in the 90-day repeated feeding study on the structural analogue, 2-(2′-hydroxy-3′,5′-di-*tert*-amylphenyl)benzotriazole, in rats (U.S. EPA, 2001). Further studies are needed to clarify the differences in the toxicological profiles between the current study and study on the analogue.

The results of the current study clearly showed sex differences in the toxic susceptibility of rats to HDBB. In males, the development of anemia and histopathologic changes in the liver, heart, kidneys, thyroid, and spleen accompanied with related blood biochemical and organ weight changes were seen. Hypertrophy of hepatocytes, decreased incidence of fatty change of hepatocytes, bile duct proliferation, increase in relative liver weight and serum A/G ratio were noted even at 0.5 mg/kg. Most of the changes were not improved after a 14-day recovery period in the highest dose group. In females, however, no anemic effects of HDBB were observed, and other effects observed in males were noted only at 12.5 mg/kg and more in females. These changes in females mostly recovered after the recovery period. These findings suggest that male rats have a nearly 25 times higher susceptibility to HDBB toxicity than female rats.

Gender-related differences in toxic susceptibility have been documented for some other substances. For example, a recent subchronic toxicity study using F344 rats showed that fluoranthene, a polycyclic aromatic hydrocarbon, had greater effects on males than females (especially on the kidneys) (Knuckles et al., 2004). In contrast, it was reported that female rats exhibited a greater

susceptibility to hypothermic effects and inhibition of hypothalamic cholinesterase by a carbamate cholinesterase inhibitor, rivastigmine (Wang et al., 2001). Such gender-related variation is also reported in humans, mostly for drugs, such as more severe adverse effects with greater improvement in response to antipsychotic drugs such as chlorpromazine and fluspirilene in women (Fletcher et al., 1994; Harris et al., 1995). The various causes of these gender differences are indicated mainly for toxicokinetic determinants. It is well-known that hepatic metabolism differs between the sexes, with males generally having higher activity than females in rats (Gad, 2006). Furthermore, gender differences in membrane transport in various organs of the body including the kidneys, liver, intestine, and brain have emerged relatively recently (Morris et al., 2003). In the case of HDBB, it is difficult to discuss the cause of the gender differences because no other data are available on toxicity, including the toxicokinetics. However, because male rats showed higher susceptibility to various effects of HDBB (on the liver, heart, blood, etc.) consistently, such differences in metabolism or transports between the sexes might increase the blood concentration of causative substances (HDBB or its metabolites) in males.

For gender differences, it goes without saying that sexual hormones play an important role. In fact, Wang et al. (2001) reported that orchidectomy completely abolished the above-mentioned sex differences in hypothalamic cholinesterase inhibition induced by rivastigmine. Because testosterone decreased cholinesterase inhibition in gonadectomized males and females, it is apparent that testosterone interferes with the effects of rivastigmine. On the other hand, estrogen has been shown to act as a dopamine antagonist (Fletcher et al., 1994; Harris et al., 1995), which is considered to contribute at least in part to sex differences in response to antipsychotic drugs. It would be interesting to investigate the role of sex steroids in the mediation of sex differences in toxic susceptibility to HDBB, too. For the metabolic enzyme cytochrome P450, involved in the metabolism of many substances, gonadal hormones are known to play an important role in regulating the expression; however, gonadal hormones do not act directly on the liver to confer the sex-dependent pattern, but rather, indirectly via the hypothalamus, which regulates the pituitary and its secretion of the polypeptide hormone, growth hormone (Waxman and Chang, 2005).

Based on the findings of this study, the NOAEL for females was concluded to be 2.5 mg kg^{-1} day^{-1} based on the induction of hypertrophy and increased mitosis of hepatocytes and degeneration and hypertrophy of the myocardium at 12.5 mg/kg. On the other hand, the NOAEL for males could not be determined because hypertrophy and decreased incidence of fatty change of hepatocytes and bile duct proliferation were noted at the lowest dose of 0.5 mg/kg. Considering the toxic effects observed at a relatively low dose and the incomplete recovery, more severe damage by the longer exposure is a concern; therefore, we

are currently performing a 52-week repeated-dose toxicity study to clarify the potential toxic effects of this chemical.

CONCLUSION

The current results showed that the oral administration of HDBB for 28 days principally affected the liver and heart, and male rats were more susceptible to the toxic effects of this chemical than female rats. The NOAEL for repeated-dose toxicity was concluded to be less than 0.5 mg kg^{-1} day^{-1} in male rats and 2.5 mg kg^{-1} day^{-1} in female rats.

ACKNOWLEDGMENT

This study was supported by the Ministry of Health, Labour and Welfare, Japan.

REFERENCES

Bartlett, M. S. (1937). Properties of sufficiency and statistical tests. *Proc. R. Soc. Lond. Ser. A* 160:268–282.

Commerce Online (2006). Product Keywords on Wujiang Dongfeng Chemical Co., Ltd. Available at http://www.commerce.com.tw/company_inside.php?ID=C0013309.

Dunnett, C. W. (1964). New tables for multiple comparisons with a control. *Biometrics* 20:482–491.

EA, MHW and MITI (Environment Agency, Ministry of Health and Welfare, and Ministry of International Trade and Industry of Japan) (1986). Partial Amendment of the Testing Methods for New Chemical Substances. Planning and Coordination Bureau, Environment Agency No. 700, Pharmaceutical Affairs Bureau, Ministry of Health and Welfare No.1039 and Basic Industries Bureaus, Ministry of International Trade and Industry No. 1014 (dated December 5, 1986).

EA, MHW and MITI (Environment Agency, Ministry of Health and Welfare, and Ministry of International Trade and Industry of Japan) (2000). Testing Facility Provided in the Article 4 in the Ordinance Prescribing Test Relating to New Chemical Substances and Toxicity Research of Designated Chemical Substances'. Planning and Coordination Bureau, Environment Agency No.41 and Environmental Health Bureau, Ministry of Health and Welfare No. 268 (dated March 1, 2000), and Basic Industries Bureaus, Ministry of International Trade and Industry No. 1 (dated February 14 2000).

Fisher, R. A. (1973). *Statistical Methods of Research Workers*, 14th ed. New York: Hapner Publishing, p. 6.

Fletcher, C. V., Acosta, E. P., Strykowski, J. M. (1994). Gender differences in human pharmacokinetics and pharmacodynamics. *J. Adolesc. Health* 15:619–629.

Gad, S. C. (2006). Metabolism. In: Gad, S. C., ed. *Animal Models in Toxicology*, 2nd ed. Boca Raton, FL: CRC Press, Taylor & Francis Group, pp. 217–247.

Glaister, J. R. (1992). Histopathology of target organs – Cardiovascular: In: *Principles of Toxicological Pathology* (Japanese version supervised by Takahashi, M.). Tokyo: Soft Science Inc., pp. 135–142.

Harris, R. Z., Benet, L. Z., Schwartz, J. B. (1995). Gender effects in pharmacokinetics and pharmacodynamics. *Drugs* 50:222–239.

Knuckles, M. E., Inyang, F., Ramesh, A. (2004). Acute and subchronic oral toxicity of fluoranthene in F-344 rats. *Ecotoxicol. Environ. Saf.* 59:102–108.

METI (Ministry of Economy, Trade and Industry of Japan) (2006). 2-(2H-1,2,3-Benzotriazole-2-yl)-4,6-di-*tert*-butylphenol. Document distributed in Committee on Safety of Chemical Substances, Chemical Substances Council, 30 June 2006. Available at http://www.meti.go.jp/committee/materials/g60705aj.html.

MHLW (Ministry of Health, Labour and Welfare, Japan) (2003). 2-(2′-Hydroxy-3′,5′-de-*tert*-butylphenyl)benzotriazole. In: *Toxicity Testing Reports of Environmental Chemicals* (Ministry of Health, Labor and Welfare ed.), Vol. 10. Tokyo: Chemicals Investigation Promoting Council, pp. 215–247.

Morris, M. E., Lee, H. J., Predko, L. M. (2003). Gender differences in the membrane transport of endogenous and exogenous compounds. *Pharmacol. Rev.* 55:229–240.

OECD (Organization for Economic Co-operation and Development) (1998). *OECD Principles on Good Laboratory Practice* (as revised in 1997). OECD Series on Principles of Good Laboratory Practice and Compliance Monitoring, No. 1. Paris: OECD.

Steel, R. D. (1959). A multiple comparison rank sum test: treatment versus control. *Biometrics* 15:560–572.

Tenkazai.com (2006). Market trend of Resin additives "Light stabilizer." Available at http://www.tenkazai.com/market.html.

U.S. EPA (2001). Robust Summaries & Test Plans: Phenolic Benzotriazoles Category, High Production Volume (HPV) Program, Available at http://www.epa.gov/chemrtk/pubs/summaries/phenbenz/c13266tc.htm.

Wang, R. H., Schorer-Apelbaum, D., Weinstock, M. (2001). Testosterone mediates sex difference in hypothermia and cholinesterase inhibition by rivastigmine. *Eur. J. Pharmacol.* 433:73–79.

Waxman, D. J., Chang, T. K. (2005). Hormonal regulation of liver cytochrome P450 enzymes. In: Ortiz de Montellano, P. R., ed. *Cytochrome P450 – Structure, Mechanism, and Biochemistry*, 3rd ed., New York: Kluwer Academic/ Plenum, pp. 347–376.

DNA REPAIR 6 (2007) 781–788

available at www.sciencedirect.com

ScienceDirect

journal homepage: www.elsevier.com/locate/dnarepair

Non-homologous end-joining for repairing I-SceI-induced DNA double strand breaks in human cells

*Masamitsu Honma**, ***Mayumi Sakuraba, Tomoko Koizumi, Yoshio Takashima, Hiroko Sakamoto, Makoto Hayashi***

Division of Genetics and Mutagenesis, National Institute of Health Sciences, 1-18-1 Kamiyoga, Setagaya-ku, Tokyo 158-8501, Japan

ARTICLE INFO

Article history:
Received 12 July 2006
Received in revised form
4 December 2006
Accepted 4 January 2007
Published on line 12 February 2007

Keywords:
DNA double strand break (DSB)
Non-homologous end-joining (NHEJ)
Homologous recombination (HR)
I-SceI
Deletion
Genomic integrity

ABSTRACT

DNA double strand breaks (DSBs) are usually repaired through either non-homologous end-joining (NHEJ) or homologous recombination (HR). While HR is basically error-free repair, NHEJ is a mutagenic pathway that leads to deletion. NHEJ must be precisely regulated to maintain genomic integrity. To clarify the role of NHEJ, we investigated the genetic consequences of NHEJ repair of DSBs in human cells. Human lymphoblastoid cell lines TSCE5 and TSCE105 have, respectively, single and double I-SceI endonuclease sites in the endogenous thymidine kinase gene (*TK*) located on chromosome 17q. I-SceI expression generated DSBs at the TK gene. We used the novel transfection system (Amaxa Nucleofector) to introduce an I-SceI expression vector into the cells and randomly isolated clones. We found mutations involved in the DSBs in the TK gene in 3% of TSCE5 cells and 30% of TSCE105 cell clones. Most of the mutations in TSCE5 were small (1–30 bp) deletions with a 0–4 bp microhomology at the junction. The others consisted of large (>60) bp deletions, an insertion, and a rearrangement. Mutants resulting from interallelic HR also occurred, but infrequently. Most of the mutations in TSCE105, on the other hand, were deletions that encompassed the two I-SceI sites generated by NHEJ at DSBs. The sequence joint was similar to that found in TSCE5 mutants. Interestingly, some mutants formed a new I-SceI site by perfectly joining the two original I-SceI sites without deletion of the broken-ends. These results support the idea that NHEJ for repairing I-SceI-induced DSBs mainly results in small or no deletions. Thus, NHEJ must help maintain genomic integrity in mammalian cells by repairing DSBs as well as by preventing many deleterious alterations.

1. Introduction

DNA double strand breaks (DSBs) are the most dangerous form of DNA damage. They can be caused by ionizing radiation (IR) or radiometric chemicals, and they can occur spontaneously during DNA replication. Other DNA damage, such as single strand breaks, easily convert to DSBs when a replication fork encounters them [1,2]. The non- or misrepair of DSBs can cause cell death or neoplastic transformation [3,4], so the accurate repair of DSBs is important for maintaining genomic integrity [5]. DSBs are generally repaired through non-homologous end-joining (NHEJ) or homologous recombination (HR) [6,7]. NHEJ joins sequences at the broken ends, which have little or no homology, in a non-conservative manner, and some genetic information is lost. HR, on the other hand, requires extensive tracts of sequence homology and is

* *Corresponding author.* Tel.: +81 3 3700 9847; fax: +81 3 3700 2348.
E-mail address: honma@nihs.go.jp (M. Honma).
1568-7864/$ – see front matter © 2007 Elsevier B.V. All rights reserved.
doi:10.1016/j.dnarep.2007.01.004

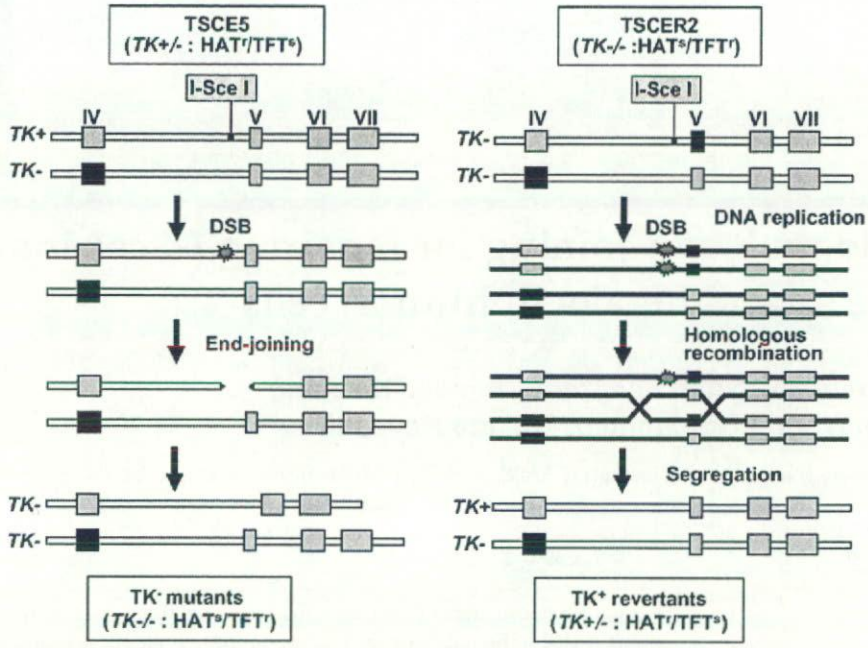

Fig. 1 – Schematic representation of the experimental system. Shadowed and closed rectangles represent the wild type and mutant exons of the *TK* gene, respectively. In TSCE5 cells, when a DSB at the I-*Sce*I site is repaired by NHEJ and causes an exon 5 deletion, TK-deficient mutants are selected in TFT medium. In TSCER2 cells, when a DSB at the I-*Sce*I site is repaired by HR, TK-proficient revertants are selected in HAT medium.

basically error-free [8]. HR is the primary DSB repair pathway in yeast and prokaryotes, but NHEJ is believed to be the primary pathway in mammalian cells [9]. HR is preferable to NHEJ because it is error-free, but NHEJ may have a different way to maintain genomic integrity.

We previously developed a human cell system to trace the fate of a DSB occurring in an endogenous single copy gene (Fig. 1) [10]. The human lymphoblastoid cell line, TSCE5, is heterozygous (+/–) and TSCER2 is compound heterozygous (–/–) for the thymidine kinase gene (*TK*), and both have an I-*Sce*I endonuclease site in intron 4. DSBs can be generated at the I-*Sce*I site by the introduction of an I-SceI enzyme expression vector. When DSBs occur at the *TK* locus, NHEJ in TSCE5 cells produces TK-deficient mutants, while HR between the alleles produces TK-proficient revertants in TSCER2 cells. Positive–negative drug selection for the TK phenotypes permits the distinction between NHEJ and HR repair mechanisms. Using the same system, we previously found that almost all I-SceI-induced DSBs in human cells are repaired by NHEJ and result in mainly 100–4000 bp deletions [10]. Drug selection, however, does not recover cells with genetic changes that are too small to influence TK function, and the resulting spectrum of mutations and reversions may be biased quantitatively as well as qualitatively.

To better understand the fate of DSBs in human cells, we randomly isolated non-selected clones after introducing DSBs and directly analyzed their DNA. A novel transfection system (Amaxa Nucleofector™) can introduce the I-SceI expression vector into most of cell population [11] and efficiently produces DSBs at the *TK* gene. With this improved method, we were able to detect cells with deletions at DSBs without drug selection and to trace the fate of DSBs without bias. We also developed a new cell line that has two I-*Sce*I sites in the *TK* gene and can be used as a model for clustering DSBs. DNA sequence analysis of the mutants in this strain revealed that both single and double DSBs were repaired predominantly by NHEJ, producing only small genetic changes, or none. We discuss how NHEJ maintains genomic integrity.

2. Materials and methods

2.1. *Human cell lines for detecting NHEJ and HR induced by a single DSB*

Human lymphoblastoid cell lines TSCE5 and TSCER2 were previously created from TK6 cells [10], which are heterozygous for a point mutation in exon 4 of the *TK* gene (*TK*+/–) (Fig. 1). TSCE5 has a 31bp DNA flagment containing the 18 bp I-*Sce*I site inserted 75bp upstream of exon 4 of the *TK*+ allele and retains TK function. TSCER2 is a TK-deficient mutant spontaneously arising from TSCE5. It has a point mutation (G:A transition) at 23bp of exon 5 of the *TK*+ allele of TSCE5. TSCER2 is compound heterozygote (*TK*–/–) for the *TK* gene. NHEJ for a DSB occurring at the I-*Sce*I site results in TK-deficient mutants in TSCE5 cells, while HR between the alleles produces TK-proficient revertants in TSCER2 cells.

2.2. *I-SceI expression and isolation of mutant clones*

We introduced the I-SceI expression vector (pCBASce) by suspending 5×10^6 cells in 0.1 ml Nucleofector solution V (Amaxa

Biosystem, Koeln, Germany) with 50 μg of uncut pCBASce vector (or without the vector as a control), following the manufacturer's recommendations. We then plated the cells into 96-microwell plates at 1 cell/well. Two weeks later, we randomly isolated single colonies and independently expanded them for DNA analysis.

We maintained the cell culture for 3 days and then seeded them into 96-microwell plates in the presence of 2.0 μg/ml trifluorothymidine (TFT) for isolating TK-deficient mutants or HAT (200 μM hypoxanthine, 0.1 μM aminopterin, 17.5 μM thymidine) for isolating TK-proficient revertants. We counted the drug-resistant colonies 2 or 3 weeks later [12] and calculated the mutation and revertant frequencies according to the Poisson distribution [13].

2.3. *Creating a cell line containing two I-SceI sites*

The targeting vector, pTK10, which we had used to make TSCE5 cells, consists of about 6 kb of the original *TK* gene encompassing exons 5, 6, and 7 and an I-SceI site in intron 4 [10]. We constructed pTK13 by inserting an additional 21 bp DNA fragment containing the 18 bp I-SceI sequence into pTK10 at the Nco I site in intron 5 (152 bp down stream of exon 5) using site-directed mutagenesis (GeneTailer, Invitrogen) (Fig. 4a). To obtain TK-revertant clones with two I-SceI sites in the *TK* gene, we transfected TSCER2 cells (5×10^6) with 20 μg of linearized pTK13 vector using the Nucleofector system. After 72 h, we seeded the cells into 96-microwell plates containing HAT. We identified one revertant clone, TSCE105, as correctly targeted and confirmed its molecular structure by DNA sequencing.

2.4. *DNA analysis*

To analyze mutations in the isolated TSCE5 and TSCE105 clones, we amplified the part of the *TK* gene containing the I-SceI sites by PCR, labeling forward primers with a fluorescent dye. We used the following primers for the I-SceI site in intron 4: forward (166F), 5′-TGG GAG AAT TAA GAG TTA CTC C-3′; reverse (196R), 5′-AGC TTC CAC CCC AGC AGC AGC T-3′. We used the following for the I-SceI site in intron 5: forward (251F), 5′-GGA TGG GCA CAG AGA CAC CA-3′; reverse (241R), 5′-CTG ATT CAC AAG CAC TGA AG-3′. For TSCE105 clones, we used 166F and 241R to amplify the regions containing both I-SceI sites. Amplification was performed by denaturation at 96 °C for 5 min, followed by 25 cycles of 96 °C for 30 s, 57 °C for 30 s, 72 °C for 30 s, and extension at 72 °C for 10 min. We analyzed the PCR products using an Agilent 2100 Bioanalyzer (Agilent Technologies, Waldbronn, Germany) and sequenced them with an ABI 310 genetic analyzer (Applied Biosystems, Foster City, CA).

3. Results and discussions

3.1. *Efficiency of the system for detecting NHEJ and HR repair of chromosomal DSBs using Amaxa nucleofection*

The lymphoblastoid cell lines, TSCE5 and TSCER2, which we previously developed, can trace the genetic consequences of chromosomal DSBs in the human genome. NHEJ for a DSB occurring at the I-SceI site results in TK-deficient mutants in TSCE5 cells, while HR between the alleles produces TK-proficient revertants in TSCER2 cells (Fig. 1) [10]. To introduce the I-SceI expression vector into the cells, we now used the Amaxa nucleofection system. The Amaxa Nucleofector™ can directly transfer DNA into the nucleus of the cells at high efficiency. It was designed for primary cells and hard-to-transfected cell lines such as the human B-cell lymphoblastoid [11,14]. Twenty-four hours after the nucleofection, approximately 65% of the transfected TSCE5 cells expressed the I-SceI enzyme, suggesting that DSBs were efficiently introduced into the cells (data not shown; Takashima et al., under submission).

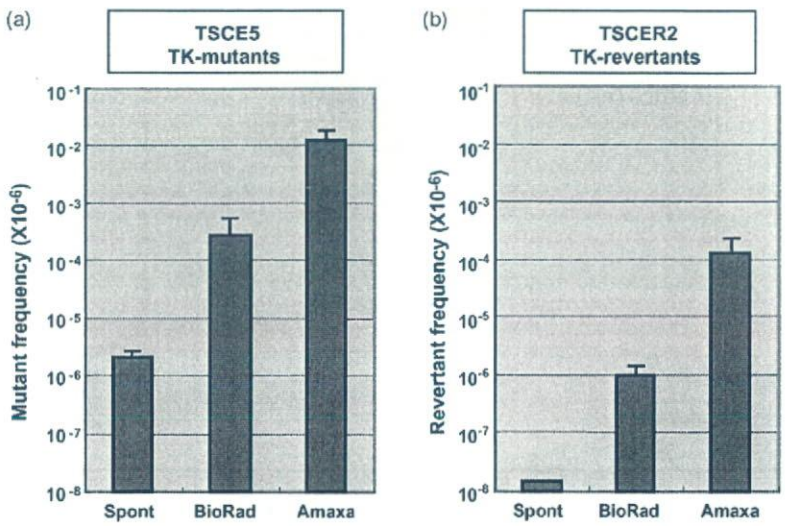

Fig. 2 – Detection of NHEJ and HR repaired DSBs using Amaxa nucleofection or BioRad electroporation. (a) Transfection of TSCE5 with the I-SceI expression vector using Amaxa nucleofection increased the TK-deficient mutant frequency more than 40-fold compared with BioRad electroporation. (b) Transfection of TSCER2 with the I-SceI expression vector using Amaxa nucleofection increased the TK-proficient revertant frequency more than 100-fold compared with BioRad electroporation.

Following Amaxa nucleofection, the mean TK mutant frequency in TSCE5 cells was 1.21%, which was more than 40-fold higher than the frequency we observed with the transfection system we had used previously (BioRad electroporation) (Fig. 2a), and the mean TK-proficient revertant frequency in TSCER2 cells was 1.22×10^{-4}, which was more than 100-fold higher than we observed previously (Fig. 2b). These results demonstrate that the Amaxa nucleofection system effciently introduced the expression vector and generated DSBs with high efficiency in the TSCE5 and TSCER2 cell lines. The relative contribution of NHEJ and HR for reparing the DSBs was 100:1. The value may be biased, however, because the drug selection assay recovers certain classes of NHEJ and HR.

3.2. *Genetic consequences of a chromosomal DSB in non-selected clones*

Because the I-*Sce*I site is inserted into intron 4 of the functional *TK* allele 75 bp upstream of exon 5, any small deletions caused by NHEJ that do not affect TK function will not be recovered as TFT-resistant mutants in the TSCE5 assay. Similarly, in the TSCER2 assay, short tract gene conversion events that do not extend to exon 5 will not be recovered as TK revertants. Thus, recovery of TK mutants and revertants by drug selection may be biased. Because nucleofection can efficiently generate DSBs at the I-*Sce*I site, however, the system enables detection of deletions and recombination in the *TK* gene without drug selection. We randomly isolated 926 transfected clones without TFT selection and directly analyzed DNAs from them. We observed that 29 (3.13%) of them had an I-*Sce*I mutation; these were usually small (<60 bp) deletions, insertions, or rearrangements (Table 1). Fig. 3 shows the DNA sequences of 21 mutants with small genetic changes. Three of them (1659, 1841, and 1893) contained a 1 bp deletion at a CCC tract within the I-*Sce*I site. Others had mostly 0–4 bp microhomologies at the junction, suggesting that the NHEJ machinery was involved. The mutant that had a 1 bp insertion at a TT tract within the I-*Sce*I site (2018) might have been generated by misalignment of the cohesive ends. The mutant that exhibited a complicated DNA rearrangement involving a 50 bp deletion combined with a 9 bp inverted sequence that was a part of deleted sequence (1614) was probably the result of sister chromatid fusion and breakage after DNA replication, as described previously [10]. Five of the mutants showed large deletions (17.2%). This fraction may correspond to the *TK* mutants in the drug selection assay. The large deletions which were commonly detected in the drug selection assay ranged from 1070 to 4030 bp, and had 4–7 bp microhomology at their junctions (data not shown) [10].

One mutant was the product of gene conversion between homologous alleles. It had lost the I-*Sce*I site and retained

Table 1 – Analysis of non-selected TSCE5 clones after I-SceI expression

Total clones	Mutant clones	Mutants (%)
926	29 (Total)	3.13
	23 (Small deletion, insertion, rearrangement; <60 bp)	2.48 (79.3)
	5 (Large deletion; >60 bp)	0.54 (17.2)
	1 (Gene conversion)	0.11 (3.4)

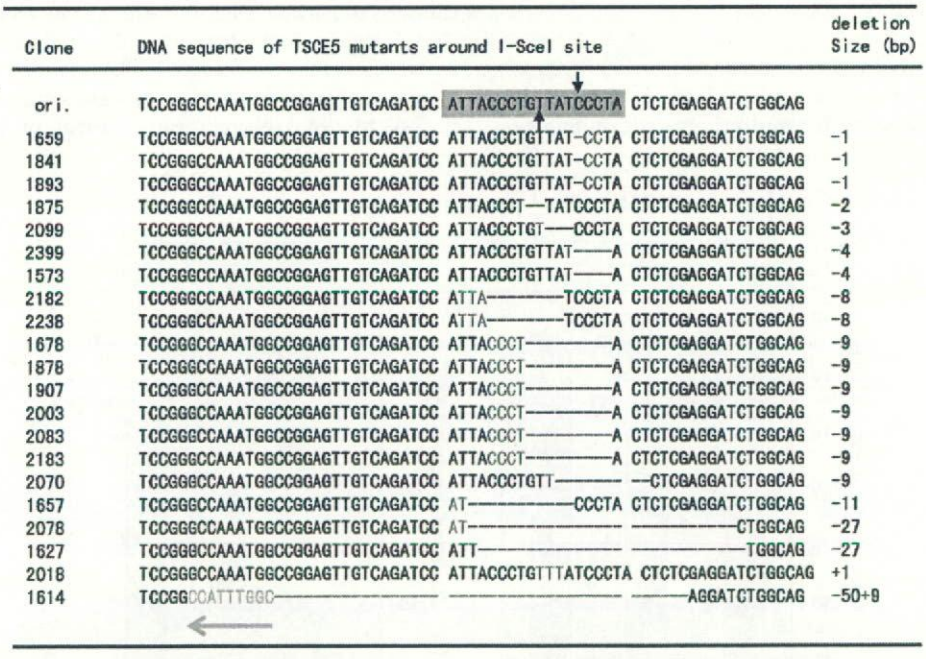

Fig. 3 – DNA sequences at the repair junction of 21 of the 26 non-selected I-SceI mutants with small (<60 bp) genetic changes in TSCE5 cells ("ori." is original sequence). The I-SceI recognition site is highlighted in orange. Arrows indicate I-SceI cleavage sites. The 1 bp deletion in the CCC tract is shown in blue and the 1 bp insertion in the TT tract is shown in green. Microhomologous sequences at junctions are shown in red. The sequence in yellow with a left arrow indicates an inverted sequence from part of a deleted sequence. (For interpretation of the references to color in this figure legend, the reader is referred to the web version of the article.)

intron 4 of the *TK* gene that had been originally connected to the I-*Sce*I site. The appearance of HR mutants was infrequent in the non-biased assay, too, suggesting that I-SceI-induced DSBs are mainly repaired by NHEJ, resulting in small deletions [10,15–17]. This does not mean that HR rarely works for DSBs, however, because our I-SceI system does not cover all HR events.

Most I-SceI systems have been developed using artificial reporter substrates based on exogenous drug-resistance or fluorescence genes and are biased in favor of detecting certain classes of deletions and recombination events [18–20]. In the present system, however, we conducted a survey of DSBs occurring in the endogenous single-copy gene, and investigated the consequences of the DSB without selection bias. We first demonstrated the mutational spectrum induced by I-SceI endonuclease in the human genome. However, it does not necessarily reflect the fate of DSBs occurring spontaneously or induced by irradiation, because our I-SceI system does not monitor sister chromatid HR, which must be the major HR pathway in mammalian cells. Other I-SceI systems setting up two tandem copies of the selective gene on the same chromosome can not also evaluate sister chromatid HR quantitatively, because both chromatids are theoretically cleaved during S/G2 phase. We may underestimate the contribution of HR in the I-SceI system.

Although the I-SceI expression vector was introduced into about 65% of the cells, the frequency of mutants at the I-*Sce*I site in the non-selection assay was still only 3.1%. Three possibilities could explain this: (1) only a small proportion of TSCE5 cells expressing the I-SceI vector may undergo a DSB, (2) most cells with DSBs may undergo apoptosis, and (3) some DSBs may go back to their original sequence by perfect joining. The last possibility would be important to the maintenance of genomic integrity following DSB repair, but its demonstration would be difficult because it is impossible to distinguish between non-cleaved and perfectly repaired I-*Sce*I sites.

3.3. *Genetic consequences of two closely separated DSBs*

To efficiently generate DSBs in the genome, we developed a cell line containing two I-*Sce*I sites in the *TK* gene. We constructed a targeting vector, pTK13, consisting of 6kb of original *TK* gene including exon 5, 6, 7 and two I-*Sce*I sites flank-

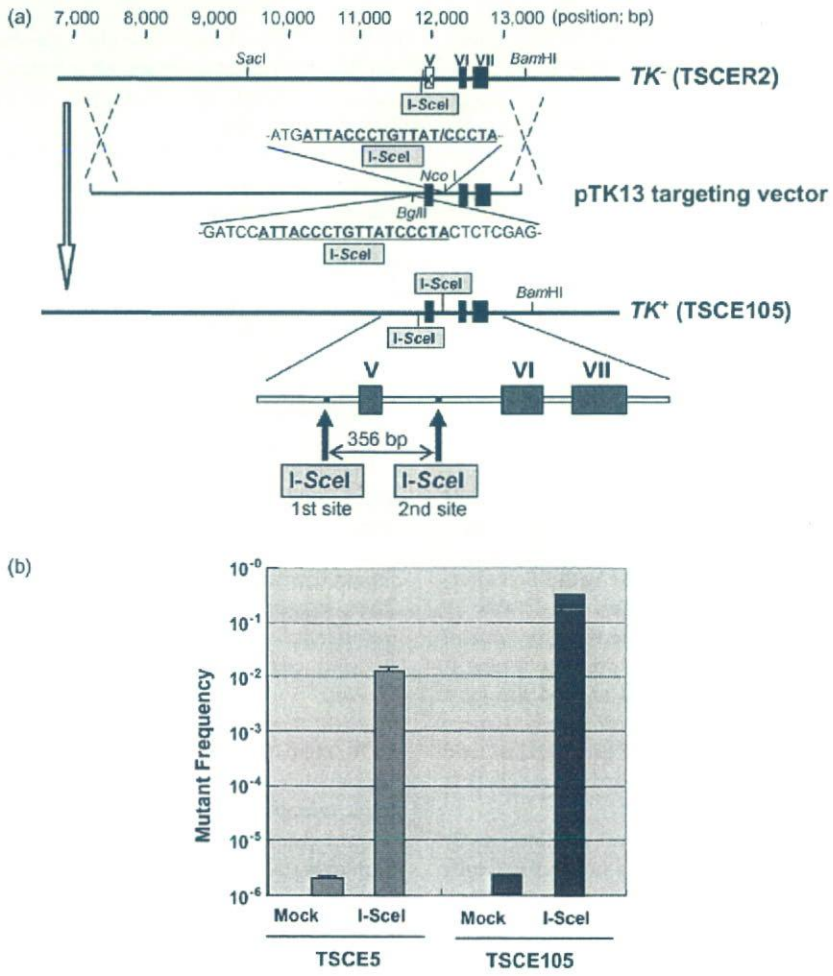

Fig. 4 – (a) Creating the TSCE105 cell line with two I-*Sce*I sites. The functional *TK* allele in the TSCE105 cell line has two I-*Sce*I recognition sites flanking exon 5, 356 bp apart. (b) The TK-deficient mutant frequency in the TSCE105 cells after introduction of DSBs by Amaxa nucleofection. The mutant frequency was 30-fold higher in TSCE105 than in TSCE5.

Table 2 – Analysis of TSCE105 mutants after I-SceI expression

Total Mutants	Type of Mutation	356bp 1st 2nd	Number of Mutants(%)
125	Only 1st I-SceI		1 (0.8)
	Only 2nd I-SceI	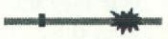	47 (38)
	Both, independent		6 (4.8)
	Both, combined		70 (56)
	Perfect joining		4
	Joining with small deletion (<60bp)		31
	Joining with large deletion (>60bp)		29
	Joining with rearrangement		6
	Recombination		1 (0.8)

ing exon 5, and transfected it to TSCER2 cells (Fig. 4a). One HAT-resistant recombinant, TSCE105, had another I-*Sce*I site at intron 5 of the *TK* gene in addtion to the original I-*Sce*I site in TSCE5. The two I-*Sce*I sites are 356 bp apart, flanking exon 5 (Fig. 4a). TSCE105 was also a *TK* heterozygote and was TFT-sensitive. When we nucleofected the I-SceI expressing vector into TSCE105, the TK-deficient mutant frequency by the TFT selection assay, surprisingly, was extremely high (31.3%) (Fig. 4b). We also examined non-selectecd clones after nucleofection. Among 283 non-selected clones, 83 (29.3%) of them had a deletion mutation involving one or both I-*Sce*I sites. This mutation frequency was about the same as the TK-deficient mutation frequency in the TFT selection assay, suggesting that most mutations in TSCE105 were deletions involving coding sequence of the *TK* gene.

To investigate the genetic changes induced by the two DSBs, we analyzed 125 mutants (42 TFT-selected and 83 non-selected) and classified them into 4 types depending on whether they occurred (1) only at the first I-*Sce*I site, (2) only at the second I-*Sce*I site, (3) independenly at both I-*Sce*I sites, or (4) at the combined first and second I-*Sce*I sites (Table 2). The majority (56%) were the last type. Interestingly, four of them joined the two I-*Sce*I sites perfectly, creating a new I-*Sce*I site. Fig. 5 shows the DNA sequences around the joint sites of 26 of the 31 mutants that had small deletions. Almost all of them had a 0–4 bp microhomology at the junction, and the sequences were similar to those found around single DSB repair sites (Fig. 3).

While a single DSB in TSCE5 cells caused predominantly small deletions, two closely occuring DSBs in TSCE105 cells were not repaired independently and caused large deletions involving the two I-*Sce*I sites, indicating that multiple DSBs enhance genetic changes qualitatively as well as quantitatively. Mammalian cells may have difficulty retaining small DNA fragments generated by multiple DSBs. High doses of ionizing irradiation, too, not only increase mutation frequency but also change the mutation type to predominantly large deletions [21,22]. The genomic changes observed in TSCE5 and TSCE105 may reflect a dosage-effect, bringing about different numbers of DSBs. In both cases, however, NHEJ is involved and injury is minimized.

The mutants with perfect joining were generated by NHEJ without exonuclease processing in which the cleaved two flanking I-*Sce*I ends simply join. Most of I-SceI-induced DSBs in TSCE5 and TSCE105 cells may be perfectly joined and create a new I-*Sce*I site. Because the I-SceI enzyme is continuously expressed for at least 48 h after nucleofection (Takashima et al., under submission), the new I-*Sce*I sites generated by perfect joining are cleaved again and again. When the DSBs are occasionally joined after exonuclease processing, they accumulate as deletional mutations and are not cleaved any more (Fig. 6). Thus, the perfect joining by NHEJ is important for repairing DSBs, at least endonuclease-induced DSBs. The perfect joining by NHEJ was also reported in other I-SceI-induced DSB systems [23,24]. Van Heemst et al. demonstrated that a blunt DSB induced by the *E. coli* transposon Tn5 were repaired without loss of nucleotides in Chinese hamster cell lines, suggesting that compatible ends precisely join without deletions [25]. The efficiency or accuracy of precise NHEJ was reduced in Ku80, DNA-PK, XRCC4, or p53 deficient cells [23–26].

NHEJ in mammalian cells involves seven components—Ku70, Ku80, DNA-PKcs, Artemis, XRCC4, Cernunnos/XLF, and Ligase IV [4,7,27–29]. Although the exact role of these proteins remains unknown, three steps have been suggested: (1) end-binding, (2) terminal processing, and (3) ligation [9]. Karanjawala et al demonstrated that defects in Artemis and DNA-PKcs, which are key components in step 2 and possess substantial nucleolytic activity, do not cause severe phenotypes or genomic instability [30]. On the other hand, deficiency of Ku (step 1) or Ligase IV (step 3) confers severe radiosensitivity or lethality [30]. Thus, the second step may not be essential in NHEJ of DSBs, especially of endonuclease-induced DSBs, because the cleaved DNA ends are ligatable

Clone	DNA sequence of TSCE105 mutants around junction site	Deletion Size (bp)
	1st site 2nd site	
perfect	TCCGGGCCAAATGGCCGGAGTTGTCAGATCC ATTACCCTGTTATCCCTA GGTCTGTGCAGACTGC	
2412	TCCGGGCCAAATGGCCGGAGTTGTCAGATCC ATTACCCTGTTATCCCTA GGTCTGTGCAAACTGC	−356 (0)
2429	TCCGGGCCAAATGGCCGGAGTTGTCAGATCC ATTACCCTGTTATCCCTA GGTCTGTGCAAACTGC	−356 (0)
2445	TCCGGGCCAAATGGCCGGAGTTGTCAGATCC ATTACCCTGTTATCCCTA GGTCTGTGCAAACTGC	−356 (0)
2465	TCCGGGCCAAATGGCCGGAGTTGTCAGATCC ATTACCCTGTTATCCCTA GGTCTGTGCAAACTGC	−356 (0)
2703	TCCGGGCCAAATGGCCGGAGTTGTCAGATCC ATTACCCTGTTAT-CCTA GGTCTGTGCAAACTGC	−357 (−1)
2650	TCCGGGCCAAATGGCCGGAGTTGTCAGATCC ATTACCCTGT----CCCTA GGTCTGTGCAAACTGC	−359 (−3)
2393	TCCGGGCCAAATGGCCGGAGTTGTCAGATCC ATTACCCTG----CCCTA GGTCTGTGCAAACTGC	−360 (−4)
2453	TCCGGGCCAAATGGCCGGAGTTGTCAGATCC ATTA--------TCCCTA GGTCTGTGCAAACTGC	−364 (−8)
2434	TCCGGGCCAAATGGCCGGAGTTGTCAGATCC AT---------ATCCCTA GGTCTGTGCAAACTGC	−365 (−9)
2345	TCCGGGCCAAATGGCCGGAGTTGTCAGATCC ATTACCCT---------A GGTCTGTGCAAACGGC	−365 (−9)
2689	TCCGGGCCAAATGGCCGGAGTTGTCAGATCC ATTACCCT---------A GGTCTGTGCAAACGGC	−365 (−9)
2714	TCCGGGCCAAATGGCCGGAGTTGTCAGATCC ATTACCCT---------A GGTCTGTGCAAACGGC	−365 (−9)
2764	TCCGGGCCAAATGGCCGGAGTTGTCAGATCC ATTACCCT---------A GGTCTGTGCAAACGGC	−365 (−9)
2444	TCCGGGCCAAATGGCCGGAGTTGTCAGATCC ATTACCCT---------A GGTCTGTGCAAACGGC	−365 (−9)
2446	TCCGGGCCAAATGGCCGGAGTTGTCAGATCC ATTACCCT---------A GGTCTGTGCAAACTGC	−365 (−9)
2424	TCCGGGCCAAATGGCCGGAGTTGTCAGATCC ATTACCCT---------A GGTCTGTGCAAACTGC	−365 (−9)
2304	TCCGGGCCAAATGGCCGGAGTTGTCAGATCC AT----------CCCTA GGTCTGTGCAAACTGC	−367 (−11)
2442	TCCGGGCCAAATGGCCGGAGTTGTCAGATCC ATTACCCTGT-------- --------GCAAACTGC	−372 (−16)
2443	TCCGGGCCAAATGTCCGGAGTTGTCAGATCC ----------TA GGTCTGTGCAAACTGC	−372 (−16)
2402	TCCGGGCCAAATGGCCGGAGTTGTCAGATCC ATTACCCTGTTAT------ ----------AACTGC	−372 (−16)
2425	TCCGGGCCAAATGGCCGGAGTTGTCAGATCC ATTACCCTGTTATC------ ----------TGC	−374 (−18)
2435	TCCGGGCCAAATGGCCGGAGTTGTCAGATCC ATTACCCTGTT------- ----------GC	−378 (−22)
2713	TCCGGGCCAAATGGCCGGAGTTGTC------- ---------- ----TGTGCAAACTGC	−384 (−28)
2735	TCCGGGCCAAATGGCCGGAGTTGTCAGATCC ---------- ----------CTGC	−378 (−22)
2405	TCCGGGCCAAATGGCCG---------- ---------- --TCTGTGCAAACGGC	−392 (−36)
2437	TCCGGGC---------- ---------- ----------AAACTGC	−409 (−53)

Fig. 5 – DNA sequences at the NHEJ repair junction around the I-SceI junction site in TSCE5 cells. "Perfect" is the DNA sequence when two I-SceI sites join perfectly and create a new I-SceI site (highlighted in orange). Sequences in black are upstream of the first I-SceI site and those in blue are downstream of the second I-SceI site. A total of 26 TSCE105 mutants with deletions combining two I-SceI sites are shown. Underlining indicates a new I-SceI recognition sequence produced by error-free NHEJ. Red indicates microhomologous sequences at junctions. (For interpretation of the references to color in this figure legend, the reader is referred to the web version of the article.)

and do not require terminal processing. Perfect joining by NHEJ probably skips the second step. Naturally occurring DSBs produced by oxidative stress, ionizing radiation, and DNA-damaging agents, however, do not have directly ligatable DNA ends and need some form of nucleolytic processing [7,9]. Their repair by NHEJ results in deletions, even if it works properly. In the present study, the size of the deletions caused by NHEJ, however, were relatively small. No recovered TSCE5 or TSCE105 mutants exhibited large deletions or translocations similar to those frequently observed

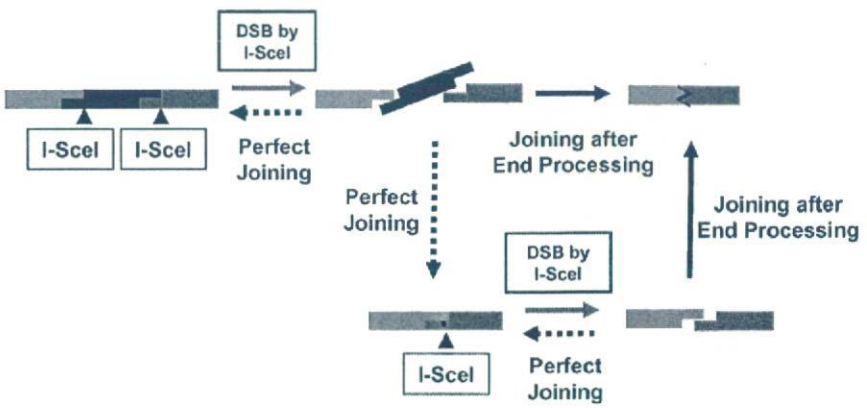

Fig. 6 – A model for NHEJ generating deletions in TSCE105 cells. When a DSB is repaired by perfect joining, an I-SceI site newly generates and is cleaved again. The rare DSB that is joined after exonuclease processing converts to a deletional mutation and accumulates in the cell population.

at the chromosome level in cancer cells [4]. This suggests that NHEJ helps maintain genomic integrity in mammalian cells by repairing DSBs as well as by preventing many deleterious alterations.

Acknowledgments

We thank Dr. Shunichi Takeda (Kyoto University) for providing the I-SceI expression vector pCBAISce. This study was supported by the Budget for Nuclear Research of the Ministry of Education, Culture, Sports, Science and Technology, based on screening and counseling by the Atomic Energy Commission.

REFERENCES

[1] K.K. Khanna, S.P. Jackson, DNA double-strand breaks: signaling, repair and the cancer connection, Nat. Genet. 27 (2001) 247–254.
[2] K.D. Mills, D.O. Ferguson, F.W. Alt, The role of DNA breaks in genomic instability and tumorigenesis, Immunol. Rev. 194 (2003) 77–95.
[3] D.C. van Gent, J.H. Hoeijmakers, R. Kanaar, Chromosomal stability and the DNA double-stranded break connection, Nat. Rev. Genet. 2 (2001) 196–206.
[4] J.H. Hoeijmakers, Genome maintenance mechanisms for preventing cancer, Nature 411 (2001) 366–374.
[5] E. Van Dyck, A.Z. Stasiak, A. Stasiak, S.C. West, Binding of double-strand breaks in DNA by human Rad52 protein, Nature 398 (1999) 728–731.
[6] S.P. Jackson, Sensing and repairing DNA double-strand breaks, Carcinogenesis 23 (2002) 687–696.
[7] K. Valerie, L.F. Povirk, Regulation and mechanisms of mammalian double-strand break repair, Oncogene 22 (2003) 5792–5812.
[8] P.A. Jeggo, DNA breakage and repair, Adv. Genet. 38 (1998) 185–218.
[9] E. Pastwa, J. Blasiak, Non-homologous DNA end joining, Acta Biochim. Pol. 50 (2003) 891–908.
[10] M. Honma, M. Izumi, M. Sakuraba, S. Tadokoro, H. Sakamoto, W. Wang, F. Yatagai, M. Hayashi, Deletion, rearrangement, and gene conversion; genetic consequences of chromosomal double-strand breaks in human cells, Environ. Mol. Mutagen. 42 (2003) 288–298.
[11] K. Maasho, A. Marusina, N.M. Reynolds, J.E. Coligan, F. Borrego, Efficient gene transfer into the human natural killer cell line, NKL, using the Amaxa nucleofection system, J. Immunol. Methods 284 (2004) 133–140.
[12] M. Honma, L.S. Zhang, M. Hayashi, K. Takeshita, Y. Nakagawa, N. Tanaka, T. Sofuni, Illegitimate recombination leading to allelic loss and unbalanced translocation in p53-mutated human lymphoblastoid cells, Mol. Cell Biol. 17 (1997) 4774–4781.
[13] E.E. Furth, W.G. Thilly, B.W. Penman, H.L. Liber, W.M. Rand, Quantitative assay for mutation in diploid human lymphoblasts using microtiter plates, Anal. Biochem. 110 (1981) 1–8.
[14] O. Gresch, F.B. Engel, D. Nesic, T.T. Tran, H.M. England, E.S. Hickman, I. Korner, L. Gan, S. Chen, S. Castro-Obregon, R. Hammermann, J. Wolf, H. Muller-Hartmann, M. Nix, G. Siebenkotten, G. Kraus, K. Lun, New non-viral method for gene transfer into primary cells, Methods 33 (2004) 151–163.
[15] J. Essers, H. van Steeg, J. de Wit, S.M. Swagemakers, M. Vermeij, J.H. Hoeijmakers, R. Kanaar, Homologous and non-homologous recombination differentially affect DNA damage repair in mice, EMBO J. 19 (2000) 1703–1710.
[16] S.P. Jackson, P.A. Jeggo, DNA double-strand break repair and V(D)J recombination: involvement of DNA-PK, Trends Biochem. Sci. 20 (1995) 412–415.
[17] J.M. Stark, M. Jasin, Extensive loss of heterozygosity is suppressed during homologous repair of chromosomal breaks, Mol. Cell Biol. 23 (2003) 733–743.
[18] P. Bertrand, D. Rouillard, A. Boulet, C. Levalois, T. Soussi, B.S. Lopez, Increase of spontaneous intrachromosomal homologous recombination in mammalian cells expressing a mutant p53 protein, Oncogene 14 (1997) 1117–1122.
[19] G.S. Boehden, N. Akyuz, K. Roemer, L. Wiesmuller, p53 mutated in the transactivation domain retains regulatory functions in homology-directed double-strand break repair, Oncogene 22 (2003) 4111–4117.
[20] C. Richardson, J.M. Stark, M. Ommundsen, M. Jasin, Rad51 overexpression promotes alternative double-strand break repair pathways and genome instability, Oncogene 23 (2004) 546–553.
[21] W.E. Bradley, A. Belouchi, K. Messing, The aprt heterozygote/hemizygote system for screening mutagenic agents allows detection of large deletions, Mutat. Res. 199 (1988) 131–138.
[22] H.L. Liber, D.W. Yandell, J.B. Little, A comparison of mutation induction at the tk and hprt loci in human lymphoblastoid cells; quantitative differences are due to an additional class of mutations at the autosomal tk locus, Mutat. Res. 216 (1989) 9–17.
[23] J. Dahm-Daphi, P. Hubbe, F. Horvath, R.A. El Awady, K.E. Bouffard, S.N. Powell, H. Willers, Nonhomologous end-joining of site-specific but not of radiation-induced DNA double-strand breaks is reduced in the presence of wild-type p53, Oncogene 24 (2005) 1663–1672.
[24] J. Guirouilh-Barbat, S. Huck, P. Bertrand, L. Pirzio, C. Desmaze, L. Sabatier, B.S. Lopez, Impact of the KU80 pathway on NHEJ-induced genome rearrangements in mammalian cells, Mol. Cell 14 (2004) 611–623.
[25] D. van Heemst, L. Brugmans, N.S. Verkaik, D.C. van Gent, End-joining of blunt DNA double-strand breaks in mammalian fibroblasts is precise and requires DNA-PK and XRCC4, DNA Rep. (Amst.) 3 (2004) 43–50.
[26] Z.E. Karanjawala, U. Grawunder, C.L. Hsieh, M.R. Lieber, The nonhomologous DNA end joining pathway is important for chromosome stability in primary fibroblasts, Curr. Biol. 9 (1999) 1501–1504.
[27] P. Ahnesorg, P. Smith, S.P. Jackson, XLF interacts with the XRCC4-DNA ligase IV complex to promote DNA nonhomologous end-joining, Cell 124 (2006) 301–313.
[28] D. Buck, L. Malivert, R. de Chasseval, A. Barraud, M.C. Fondaneche, O. Sanal, A. Plebani, J.L. Stephan, M. Hufnagel, F. le Deist, A. Fischer, A. Durandy, J.P. de Villartay, P. Revy, Cernunnos, a novel nonhomologous end-joining factor, is mutated in human immunodeficiency with microcephaly, Cell 124 (2006) 287–299.
[29] S. Burma, D.J. Chen, Role of DNA-PK in the cellular response to DNA double-strand breaks, DNA Rep. (Amst.) 3 (2004) 909–918.
[30] Z.E. Karanjawala, N. Adachi, R.A. Irvine, E.K. Oh, D. Shibata, K. Schwarz, C.L. Hsieh, M.R. Lieber, The embryonic lethality in DNA ligase IV-deficient mice is rescued by deletion of Ku: implications for unifying the heterogeneous phenotypes of NHEJ mutants, DNA Rep. (Amst.) 1 (2002) 1017–1026.

Available online at www.sciencedirect.com
ScienceDirect
Mutation Research 634 (2007) 235–240
Genetic Toxicology and Environmental Mutagenesis
www.elsevier.com/locate/gentox
Community address: www.elsevier.com/locate/mutres

Short communication

Sensitivity of the erythrocyte micronucleus assay: Dependence on number of cells scored and inter-animal variability

Grace E. Kissling [a,*], Stephen D. Dertinger [b], Makoto Hayashi [c], James T. MacGregor [d]

[a] *National Institute of Environmental Health Sciences, Research Triangle Park, NC 27709, United States*
[b] *Litron Laboratories, Rochester, NY 14623, United States*
[c] *National Institute of Health Sciences, Tokyo 158-8501, Japan*
[d] *Toxicology Consulting Services, Arnold, MD 21012, United States*

Received 21 May 2007; received in revised form 27 July 2007; accepted 30 July 2007
Available online 6 August 2007

Abstract

Until recently, the *in vivo* erythrocyte micronucleus assay has been scored using microscopy. Because the frequency of micronucleated cells is typically low, cell counts are subject to substantial binomial counting error. Counting error, along with inter-animal variability, limit the sensitivity of this assay. Recently, flow cytometric methods have been developed for scoring micronucleated erythrocytes and these methods enable many more cells to be evaluated than is possible with microscopic scoring. Using typical spontaneous micronucleus frequencies reported in mice, rats, and dogs we calculate the counting error associated with the frequency of micronucleated reticulocytes as a function of the number of reticulocytes scored. We compare this counting error with the inter-animal variability determined by flow cytometric scoring of sufficient numbers of cells to assure that the counting error is less than the inter-animal variability, and calculate the minimum increases in micronucleus frequency that can be detected as a function of the number of cells scored. The data show that current regulatory guidelines allow low power of the test when spontaneous frequencies are low (e.g., ≤0.1%). Tables and formulas are presented that provide the necessary numbers of cells that must be scored to meet the recommendation of the International Working Group on Genotoxicity Testing that sufficient cells be scored to reduce counting error to less than the inter-animal variability, thereby maintaining a more uniform power of detection of increased micronucleus frequencies across laboratories and species.

Keywords: Erythrocyte micronucleus assay; Flow cytometry; Binomial counting error; Inter-animal variability; Power calculation

1. Introduction

The ability of the *in vivo* erythrocyte micronucleus assay to detect small increases in the spontaneous background frequency of micronucleated cells in a group of animals (or study subjects) is limited by either the binomial counting error, when the number of cells scored gives small numbers of scored events (micronucleated cells) [1–4], or by inter-animal variation, when that variation is so large that it obscures a small, but real, increase. Furthermore, the sensitivity to detect small increases in the micronucleus frequency in an individual animal is limited at small micronucleus counts by the binomial counting error and at higher counts by the spontaneous variability in that individual animal over the time span in

* Corresponding author. Tel.: +1 919 541 1756; fax: +1 919 541 4311.
E-mail address: kissling@niehs.nih.gov (G.E. Kissling).

1383-5718/$ – see front matter © 2007 Elsevier B.V. All rights reserved.
doi:10.1016/j.mrgentox.2007.07.010